PHYSICAL REVIEW D VOLUME 23, NUMBER 11 1 JUNE 1981

Quark models for hadronic reactions. Nucleon-nucleon scattering

T. R. Mongan
84 Marin Avenue, Sausalito, California 94965
(Received 23 April 1980; revised manuscript received 18 August 1980)

A model for the development of scattered quarks into final-state hadrons is extended for application to hadronic reactions, focusing on nucleon-nucleon scattering in particular. Numerical calculations show that the model reproduces the main features of experimental data on secondary-hadron production in low-transverse-momentum nucleon-nucleon scattering at c.m. energies above about 3 GeV, including the variation of σ_{el}/σ_{tot} with energy, the average charged-hadron multiplicity, the moments of the charged-hadron multiplicity distribution, and the longitudinal-momentum distribution of final-state hadrons. In anticipation of the future availability of higher-energy nucleon colliding-beam machines, charged-hadron multiplicities are estimated for c.m. energies up to 2000 GeV.

INTRODUCTION

Based on regularities in the properties of hadron families and the results of deep-inelastic lepton-hadron and large-momentum-transfer hadron-hadron scattering, many physicists believe that hadrons are made up of elementary fermions called quarks, even though these quarks have never been observed in isolation.

If hadrons are composed of quarks, the generation of secondary hadrons in hadronic scattering reactions must be a two-stage process. The first stage involves the scattering of the quarks contained within the colliding hadrons. A detailed model of the force between quarks is needed to calculate the cross section and angular distribution of the scattered quarks. A candidate non-Abelian gauge field theory, quantum chromodynamics (QCD), has been suggested to describe the interaction of quarks through the exchange of massless vector bosons called gluons. Because this field theory is asymptotically free, perturbation calculations can be performed for elementary processes at short distances (large momentum transfers). It is hoped that QCD will lead to estimates of the quark cross sections and angular distributions, at least at high energies. Then some form of additivity should lead to estimates for the hadronic total cross sections.

The second stage in a secondary-hadron production process involves the development of the scattered quarks into final-state hadrons (hadronization). This process is poorly understood at present. QCD calculations of hadronization are likely to be extremely difficult, involving soft processes in a region where the coupling constant is too large to allow a convergent perturbation expansion.

Consequently, it seems appropriate to find out if a conceptually simple approach for directly calculating the properties of the hadronization process can reproduce the main features of the experimental data on secondary-hadron production, namely jet structure, the multiplicity distribution of final-state hadrons, the distribution of final-state hadron momenta along the jet direction, and the fraction of inelastic scattering events in hadron-hadron scattering.

If a relatively simple picture of hadronization reproduces the main features of the experimental data, one can conclude optimistically that QCD will give results in agreement with experiment if it can be shown globally that the decay of excited quark matter into hadrons has certain simple overall features in agreement with the postulated picture. Detailed field-theoretical calculations of the decay amplitudes would then be unnecessary. Alternatively, one could conclude that experimental data on the evolution of scattered quarks into hadrons will not provide a particularly stringent test of QCD.

For this reason, I have been working on a simple calculable model for the evolution of excited quark-antiquark ($Q\bar{Q}$) pairs into final-state hadrons. This model postulates that an excited $Q\bar{Q}$ pair (fireball) decays isotropically in its own rest frame into final-state hadrons with the decay multiplicity given by a (truncated) Poisson distribution. The average number of secondary hadrons produced by fireball decay is found by dividing the fireball invariant mass by a fixed quantity, the average energy of a secondary hadron in the fireball rest frame. Therefore, although fireballs can decay into varying numbers of final-state hadrons with correspondingly varying momenta transverse to the momentum of the fireball c.m., the average value of the transverse momentum of the secondary hadrons with respect to the fireball c.m. momentum remains constant. Furthermore, the average number of secondary hadrons increases linearly with the invariant mass of the fireball.

This description of hadronization has already been successfully applied to hadron production in

e^+e^- annihilation[1,2] and in lepton-hadron scattering (as will be reported in a subsequent paper) where a straightforward approach to the conversion of the scattered quark into an excited $Q\bar{Q}$ pair is applicable. If such a description of hadronization has any general utility, it must also be successful in describing the main features of secondary-hadron production in hadronic-scattering reactions.

Since the great majority of final-state hadrons in a hadronic-scattering event have low momentum transverse to the beam direction and a successful description of the angular distribution of final-state hadrons is likely to require a detailed model of the force between colliding quarks, I shall specialize to the case of hadrons scattering at low transverse momentum.

To calculate the multiplicity and rapidity distribution of final-state hadrons produced in a hadronic scattering reaction, the fireball-decay model must be extended by incorporating a model which describes when and how fireballs are created in hadron-hadron scattering and determines the longitudinal momentum and invariant mass of the fireball. This fireball-generation model will be based on a constituent-quark picture of hadrons similar to that used by Altarelli, Cabibo, Maiani, and Petronzio.[3]

In a previous paper,[4] I developed a method for calculating multiplicity distributions in proton-proton scattering based on the simple picture of isotropic fireball decay which was reasonably successful in reproducing the main features of low-transverse-momentum experimental data, However, two criticisms could be leveled at this approach.

(1) The distribution of quark momenta within the colliding hadrons was not taken into account. Instead, it was assumed that each constituent quark carried $\frac{1}{3}$ of the proton's momentum. This leads to a vanishing density of secondary hadrons at fixed rapidity for asymptotic values of the c.m. energy, which seems to be at variance with the present trend of experimental data.

(2) Two different types of hadronic fireballs were postulated to prevent the leading nucleon from appearing with only certain discrete fractions of the incident hadron's momentum. This complication is related to the inadequate treatment of the distribution of quark momentum within the colliding hadrons.

In this paper, I combine the fireball-decay model with a fireball-generation model to develop a readily calculable model for the multiplicity and rapidity distributions of low-transverse-momentum secondary hadrons generated in high-energy nucleon-nucleon scattering. This composite model takes account of the distribution of quark momenta within the colliding nucleons and involves the generation and decay of only one type of fireball. The inputs to the model are directly related to experimentally measured quantities. Although no attempt was made to search for optimum input values, the model is successful in reproducing the main features of the experimental data on low-transverse-momentum hadron production in nucleon-nucleon scattering using reasonable values of the input parameters. This success indicates that many aspects of the experimental data on secondary-hadron production may simply reflect the quark content of hadrons, energy-momentum conservation, and a simple decay process for secondary-hadron fireballs. It also suggests that the necessary bridge between QCD and the experimental data on hadron-jet production can be built by showing that an excited $Q\bar{Q}$ pair (fireball) in QCD tends to decay isotropically in its own rest frame into final-state hadrons with a Poisson distribution in multiplicity and an average decay multiplicity related to the fireball invariant mass by a fixed value of the average energy of a secondary hadron in the fireball rest frame.

Because the total nucleon-nucleon cross section can be readily parametrized , this model may have direct practical utility for calculating cosmic-ray cascades and the multiplicity and rapidity distributions anticipated at energies presently inaccessible in the laboratory. The resulting information should be useful in designing cosmic-ray experiments and experiments at future high-energy accelerators. Furthermore, large deviations of the experimental data from the calculated values could provide an indication of new effects which are not present at currently accessible energies. The fact that the charged multiplicity in this model grows as $E^{1/4}$ (where E is the incident laboratory nucleon-beam energy), as suggested by the cosmic-ray data, favors its use for estimating multiplicity and rapidity distributions at energies beyond those accessible by present accelerators.

I have performed calculations with several approximate versions of the model to show that the desirable features of the model are not destroyed by approximations which might be used to speed calculations in complex applications. I have also included some brief remarks regarding the extension of my model for hadronization to particle production in large-transverse-momentum jets.

ASSUMPTIONS

Consider two infinite-momentum hadrons col-

liding in the c.m. frame[5] and assume that inelastic collisions involve only longitudinal momentum transfer.[6] The fireball generation model is then based on the following assumptions.

(1) Each colliding hadron is composed of constituent quarks, and hadronic reactions are dominated by events in which one quark in the beam hadron (the beam quark) scatters off one quark in the target hadron (the target quark). This is the standard assumption of the additive quark model for high-energy hadronic scattering.[7] The remaining constituent quarks act as spectators, retaining their initial fraction of the incident hadron's momentum.

The probability that a constituent quark carries a fraction x of the momentum of the colliding hadron is (in the infinite-momentum frame) determined by a function $f^c(x)$ which satisfies

$$\int_0^1 f^c(x)\,dx = 1 , \tag{1a}$$

$$\int_0^1 x f^c(x)\,dx = 1/n_Q , \tag{1b}$$

where n_Q is the number of constituent quarks in the colliding hadron.

(2) Each constituent quarks consists of a valence quark plus an accompanying (virtual) color gluon cloud.[3] The probability of a constituent quark (in a hadron moving at infinite momentum) containing a valence quark plus k gluons is given by a Poisson distribution[8]

$$P_Q(k) = \mu_h^{\,k} e^{-\mu_h}/k! , \tag{2}$$

where μ_h is the average number of virtual gluons accompanying a valence quark in a hadron h moving at infinite momentum.

The probability that the valence quark within a constituent quark containing k gluons carries a fraction y of the constituent quark's momentum is determined (in the infinite-momentum frame) by functions $g_k(y)$ which satisfy

$$\int_0^1 g_k(y)\,dy = 1 , \tag{3a}$$

$$\int_0^1 y g_k(y)\,dy = 1/(2k+1) . \tag{3b}$$

Condition (3b) implies that, as suggested by the equilibrium gluon $\rightleftharpoons$ quark-antiquark ($Q\bar{Q}$) pair, a gluon carries on the average twice as much momentum as a bare quark.[9]

(3) The force between two colliding quarks can be modeled by an implusive force in the c.m. frame at very high energies.[10] If the (longitudinal) impulse is denoted Δ, the four-momentum transfer is the minimum compatible with the longitudinal momentum transfer (impulse) Δ. Consequently, in inelastic collisions, where some of the kinetic energy of the colliding hadrons goes to produce secondary hadrons, the total c.m. momentum p' of the system of final-state hadrons arising from the beam (or target) hadron is given by

$$p' = p - \Delta , \tag{4}$$

where p is the c.m. momentum of the incident hadrons. In elastic collisions, of course, the direction of the incident hadron's c.m. momentum is changed, but the magnitude is unaltered.

(4) The incident beam (or target) constituent quark may consist, with probability $P_Q(0)$, of a valence quark unaccompanied by virtual gluons. If this is the case, and the scattered quark does not emit gluons as it recoils from the collision, no secondary hadrons are produced in association with the scattered quark. The probability of an incident constituent quark consisting of an unaccompanied valence quark emitting zero gluons in a scattering event (i.e., the probability of such a scattered quark appearing as an unaccompanied valence quark after the scattering event) equals $P_Q(0)$, the probability that the incident constituent quark is an unaccompanied valence quark.

If secondary quarks are produced by neither the beam nor the target quark (because both of the incident constituent quarks are unaccompanied valence quarks and neither of these unaccompanied valence quarks emit gluons while recoiling from the scattering) the event is an elastic scattering.

The incident beam (or target) constituent quark may consist, with probability $P_Q(k)$, of a valence quark plus k virtual gluons. In this case, the collision breaks up the constituent quark and converts the gluons into quark-antiquark ($Q\bar{Q}$) pairs. The spectator quarks pick up a bare quark with the appropriate color charge out of the fragments of the fragments of the scattered constituent quark to form a "leading" hadron. The probability that the bare quark picked up by the spectators to form the leading hadron carries a fraction y of the momentum of the scattered constituent quark is determined by the functions $g_k(y)$ satisfying Eq. (3). The remaining k $Q\bar{Q}$ pairs which are fragments of the scattered constituent quark are the precursors of a fireball of secondary hadrons.

On the other hand, if the incident beam (or target) constituent quark consists of an unaccompanied valence quark, the valence quark may, when recoiling from the collision, emit k gluons which are then instantly converted into $Q\bar{Q}$ pairs. The probability of a colliding constituent quark which

consists of an unaccompanied valence quark emitting k gluons in a scattering event (i.e., the probability of a colliding unaccompanied valence quark generating a quark plus k $Q\bar{Q}$ pairs after the collision) equals $P_Q(k)$, the probability of an incident constituent quark containing a valence quark plus k virtual gluons. The spectator quarks again form a leading hadron by picking up a bare quark with the appropriate color charge out of the quarks and antiquarks created from the scattering of the initially unaccompanied valence quark. Once again, the probability that the bare quark picked up by the spectators to form the leading hadron carries a fraction y of the momentum of the scattered quark is determined by the functions $g_k(y)$ satisfying Eq. (3), and the remaining $k Q\bar{Q}$ pairs generated by the scattered quark are the precursors of a fireball of secondary hadrons.

Although elaborations are obviously possible, the two production mechanisms outlined above are treated similarly in this model and there is no difference in the subsequent evolution of the fireballs into secondary hadrons.

The fireball-decay model assumes that the secondary-hadron fireballs emit hadrons isotropically in the fireball c.m. frame, just as in my model for e^+e^- annihilation into hadrons.[1] Each fireball creates at least one hadron, and the number n of additional hadrons produced follows a truncated Poisson distribution[11]

$$P_F(n;m_F^*)=\alpha[\xi(m_F^*)]^n e^{-\xi(m_F^*)}/n!, \quad n\leq\frac{m_F^*}{m_\pi}-1, \tag{5a}$$

$$P_F(n;m_F^*)\equiv 0, \quad n>\frac{m_F^*}{m_\pi}-1 . \tag{5b}$$

All secondary hadrons are assumed to be pions, the average number $\xi(m_F^*)$ of additional pions produced by a fireball with invariant mass m_F^* is

$$\xi(m_F^*)=[m_F^*/(p_H^2+m_\pi^2)^{1/2}]-1 \tag{6}$$

and $(p_H^2+m_\pi^2)^{1/2}$ is the average energy needed to produce a pion in the fireball c.m. frame. The average energy required to produce a pion, $(p_H^2+m_\pi^2)^{1/2}$, is determined by the pion mass m_π and $|\vec{p}_H|$ which is the average magnitude of the momentum of a produced hadron in the fireball c.m. frame.[12] The normalization constant α is given by

$$\alpha^{-1}=\sum_{n=0}^{n_{\max}}[\xi(m_F^*)]^n e^{-\xi(m_F^*)}/n! ,$$

where $n_{\max}$ is the largest integer less than or equal to $(m_F^*/m_\pi)-1$.

These assumptions allow the development of a composite model for secondary-hadron production in infinite-momentum hadronic scattering. The following additional, and somewhat arbitrary, assumption is made to carry out calculations at finite momenta. If the c.m. three momenta $x_B p$ and $x_T p$ of both of the colliding constituent quarks is less than Δ, the three-momentum transferred in the collision is equal to the largest of $x_B p$ and $x_T p$.

MODEL INPUTS FOR NUCLEON-NUCLEON SCATTERING

In this model, the probability of elastic scattering is the probability $P_Q{}^4(0)$ that neither the beam nor the target constituent quarks produce secondary hadrons. At high energies, the ratio σ_{el}/σ_{tot} has a constant value of about 0.175 in nucleon-nucleon scattering. If all constituent quarks in the nucleons are treated the same,

$$P_Q{}^4(0)=e^{-4\mu_n}=0.175. \tag{7}$$

Therefore, the average number μ_n of gluons in a constituent quark within a nucleon moving with infinite momentum is $\mu_n=0.436$.

The average transverse momentum of secondary pions in this model is

$$\langle|\vec{p}_T|\rangle\approx(\tfrac{2}{3})^{1/2}|\vec{p}_H| . \tag{8}$$

If $|\vec{p}_H|$ is taken as 440 MeV/c, the average transverse momentum of secondary pions is 360 MeV/c, as suggested by experimental data.

The work of Malone and Lo[13] indicates that the average longitudinal three-momentum transfer Δ in nucleon-nucleon collisions at a c.m. energy of 45 GeV is 1.8 GeV/c, and this value was used in all calculations.

The form of the function $f^c(x)$ is chosen as $\sim x^{a-1}(1-x)^{b-1}$. Using the relations

$$\int_0^1 x^{a-1}(1-x)^{b-1}dx=\frac{\Gamma(a)\Gamma(b)}{\Gamma(a+b)}$$

and

$$\Gamma(a+1)=a\Gamma(a) ,$$

it is clear that conditions (1) require $(n_Q-1)a=b$. Because $\mu_n=0.436$, the probability of a constituent quark consisting of an unaccompanied valence quark is $P_Q(0)=0.647$. Since the deep-inelastic-scattering data indicate[14] that F_2^{ep} behaves approximately as $(1-x)^3$ when $x\to 1$, I chose $b=4$ for the function $f^c(x)$. Then, since $n_Q=3$ for a nucleon, $a=2$ and the normalization condition (1a) requires that

$$f^c(x)=20x(1-x)^3 . \tag{9}$$

Following Altarelli *et al.*,[3] the functions $g_k(y)$ were chosen as

$$g_k(y) = \frac{\Gamma(k+\frac{1}{2})}{\Gamma(\frac{1}{2})\Gamma(k)} \frac{(1-y)}{\sqrt{y}}^{k-1}$$
$$= A_k \frac{(1-y)}{\sqrt{y}}^{k-1} . \quad (10)$$

This form for $g_k(y)$ will introduce the $1/\sqrt{x}$ behavior[15] of the nucleon structure functions at small x when a prescription similar to that developed by Altarelli *et al.*[3] is used to generate the nucleon structure functions from the function $f^c(x)$ and $g_k(y)$.

MODEL DEVELOPMENT

Consider the colliding constituent quark in one of the incident hadrons. The probability, in the infinite-momentum frame, of this constituent quark consisting of a valence quark plus k virtual gluons is given by the Poisson distribution (2), which satisfies $1 = \Sigma_{k=0}^{\infty} P_Q(k)$. If this equation is rewritten as

$$1 = P_Q(0) + \sum_{k=1}^{\infty} P_Q(k)$$
$$\equiv P_Q(0) + [1 - P_Q(0)] \quad (11)$$

the first term $P_Q(0) = e^{-\mu_k}$ gives the probability that the incident constituent quark is an unaccompanied valence quark, while the second term gives the probability that the incident constituent quark contains gluons and will consequently break up during the collision to create a secondary-hadron fireball.

Since the probability of an unaccompanied valence quark emitting k gluons during a collision was assumed to equal $P_Q(k)$, Eq. (11) can again be rewritten as

$$1 = P_Q(0)\{P_Q(0) + [1 - P_Q(0)]\} + [1 - P_Q(0)]$$
$$= P_Q{}^2(0) + P_Q(0)[1 - P_Q(0)] + [1 - P_Q(0)] , \quad (12)$$

where the first term gives the probability $P_Q{}^2(0) = e^{-2\mu_k}$ that no secondary hadrons are created from the colliding quark. The second term in (12) is the probability of producing secondary hadrons from gluons emitted during the collision by a colliding constituent quark which was initially an unaccompanied valence quark. The third term in (12) is the probability that a secondary-hadron fireball is produced by the breakup of a colliding constituent quark which initially contains one or more virtual gluons. Equation (12) can also be written as

$$1 = P_Q{}^2(0) + [1 + P_Q(0)] \sum_{k=1}^{\infty} P_Q(k) , \quad (13)$$

where the two terms give the probability that a colliding constituent quark does or does not generate a fireball of secondary hadrons.

Since one constituent quark in each colliding hadron participates in a high-energy hadronic reaction, the probability of different types of hadronic scattering events is determined by the product of expressions such as Eq. (13) for the beam (B) and target (T) quarks:

$$1 = P_{QB}{}^2(0) P_{QT}{}^2(0) + P_{QB}{}^2(0)[1 + P_{QT}(0)] \sum_{k=1}^{\infty} P_{QT}(k)$$
$$+ P_{QT}{}^2(0)[1 + P_{QB}(0)] \sum_{k=1}^{\infty} P_{QB}(k)$$
$$+ \left\{[1 + P_{QB}(0)] \sum_{k'=1}^{\infty} P_{QB}(k')\right\}$$
$$\times \left\{[1 + P_{QT}(0)] \sum_{k=1}^{\infty} P_{QT}(k)\right\} . \quad (14)$$

The first term in Eq. (14) is the probability of elastic scattering. The next two terms in Eq. (14) are the probability of one-fireball events, where the fireballs are generated by the target and beam quarks, respectively. The last term in Eq. (14) is the probability of two-fireball events.

From Eq. (5), the probability of producing $n+1$ secondary hadrons (pions) is determined by the pion mass m_π, the average pion momentum in the fireball rest frame, and the invariant mass of the fireball m_F^*. The fireball mass is in turn determined, through kinematics, by the fraction x of the incident hadron's momentum carried by the colliding constituent quark and the fraction y of the momentum of the scattered constituent quark system which is carried by the bare quark picked up to form the leading hadron.

Experiment generally measures charged-particle production, and since charge conservation requires that charged particles are produced in pairs, it is convenient to develop the model in terms of the number of charged-hadron pairs produced in addition to the two initial colliding hadrons (protons). Denote the probability of the fireball in a single-fireball event producing n charged-hadron pairs by $P_c[n, m_F^*(k, x_D, x_P, y_P)]$. Then, since the probability of a pion pair being charged is $\frac{2}{3}$, the probability of producing n charged-hadron (pion) pairs from the fireball is

$$P_c[n, m_F^*(k, x_D, x_P, y_P)]$$
$$= \sum_{i=n}^{\infty} (\tfrac{2}{3})^n (\tfrac{1}{3})^{i-n} \left[\frac{i!}{n!(i-n)!}\right]$$
$$\times [P_F(2i, m_F^*) + P_F(2i-1, m_F^*)] . \quad (15)$$

In Eq. (15), $P_F(n, m_F^*)$ is obtained from Eq. (5), and I have explicitly indicated the dependence of the fireball mass m_F^* on the number k of gluons which are precursors of the hadronic fireball,

the fraction x_D and x_P of the momentum of the colliding hadrons carried by the dormant (D) and producing (P) constituent quarks and the fraction y_P of the momentum of the producing constituent quark system after scattering which is carried by the bare quark picked up by the spectators to form the leading hadron in the hadronic system associated with the fireball.

In a similar fashion, the probability of one of the fireballs in a two-fireball event producing n secondary charged-hadron pairs is denoted by $P_F[n, m_F^*(k, x_B, y_B, x_T, y_T)]$, where the subscripts B and T indicate the beam and target, respectively, and is calculated in the same way as indicated in Eq. (15). Then, using Eqs. (1a), (3a), and (15), Eq. (14) can be put in the form

$$
\begin{aligned}
1 = {} & P_{QB}^2(0)P_{QT}^2(0) \\
& + P_{QB}^2(0)[1+P_{QT}(0)]\int_0^1\int_0^1 dx_B\,dx_T f^c(x_B)f^c(x_T)\sum_{k=1}^{\infty} P_{QT}(k)\int_0^1 dy_T g_k(y_T)\sum_{n=0}^{n_{\max}/2} P_c[n, m_F^*(k, x_B, x_T, y_T)] \\
& + P_{QT}^2(0)[1+P_{QB}(0)]\int_0^1\int_0^1 dx_B\,dx_T f^c(x_B)f^c(x_T)\sum_{k=1}^{\infty} P_{QB}(k)\int_0^1 dy_B g_k(y_B)\sum_{n=0}^{n_{\max}/2} P_c[n, m_F^*(k, x_T, x_B, y_B)] \\
& + [1+P_{QB}(0)][1+P_{QT}(0)]\int_0^1\int_0^1 dx_B dx_T f^c(x_B) f^c(x_T) \\
& \qquad \times\sum_{k=1}^{\infty}\sum_{l=1}^{\infty} P_{QB}(k)P_{QT}(l)\int_0^1\int_0^1 dy_B dy_T\, g_k(y_B)g_l(y_T)\sum_{n=0}^{n_{\max}/2} P_c[n, m_{BF}^*(k, x_B, y_B, x_T, y_T)] \\
& \qquad \times\sum_{m=0}^{m_{\max}/2} P_c[m, m_{TF}^*(l, x_B, y_B, x_T, y_T)] . \qquad (16)
\end{aligned}
$$

Equation (16), which sums the probabilities of different final states of a hadronic scattering event, forms the basis for my model. Denote the probability of producing b secondary charged hadron pairs in addition to the charges carried on the colliding hadrons by $P'_{ch}(b)$. Then

$$
\sum_{b=0}^{N_{\max}} P'_{ch}(b) = 1 , \qquad (17)
$$

where $N_{\max} = (E_{c.m.} - 2m_N)/2m_{\pi 0}$ is the upper limit on the number of secondary hadron pairs which can be produced if $E_{c.m.}$ is the total c.m. energy of the nucleon-nucleon collision and m_N is the nucleon mass. Then, rearranging Eq. (16) and convoluting the probabilties for producing charged final state hadron pairs from two-fireball events yields

$$
\begin{aligned}
P'_{ch}(b) = {} & \delta_{b0}P_{QB}^2(0)P_{QT}^2(0) + \int_0^1\int_0^1 dx_B dx_T f^c(x_B)f^c(x_T) \\
& \times\Big\{P_{QB}^2(0)[1+P_{QT}(0)]\sum_{k=1}^{\infty} P_{QT}(k)\int_0^1 dy_T g_k(y_T)P_c[b, m_F^*(k, x_B, x_T, y_T)] \\
& + P_{QT}^2(0)[1+P_{QB}(0)]\sum_{k=1}^{\infty} P_{QB}(k)\int_0^1 dy_B g_k(y_B)P_c[b, m_F^*(k, x_T, x_B, y_B)] \\
& + [1+P_{QB}(0)][1+P_{QT}(0)]\sum_{k=1}^{\infty}\sum_{l=1}^{\infty} P_{QB}(k)P_{QT}(l)\int_0^1\int_0^1 dy_B dy_T g_k(y_B)g_l(y_T) \\
& \qquad \times\sum_{a=0}^{b} P_c[b-a, m_{BF}^*(k, x_B, y_B, x_T, y_T)] \\
& \qquad \times P_c[a, m_{TF}^*(l, x_B, y_B, x_T, y_T)]\Big\} . \qquad (18)
\end{aligned}
$$

Since charge is conserved and the colliding hadrons in a pp collision are both charged, the probability $P_{ch}(n)$ of finding n charged hadrons in the final state of a pp scattering event is $P_{ch}(n) = P_{ch}(2b+2) = P'_{ch}(b)$ and it is this multiplicity distribution which serves as the basis for experimental comparisons. Many experiments involve the properties of the multiplicity distribution of

the charged hadrons produced in inelastic collisions. The average number of charged hadrons produced in the inelastic scattering of two positively (or negatively) charged hadrons is given by

$$\langle n\rangle = \left[\sum_{n\geq 2} nP_{\rm ch}(n) - 2P_{\rm el}\right]/(1-P_{\rm el}) \tag{19}$$

and the higher moments of the distribution are determined by

$$\langle n^k\rangle = \left[\sum_{n\geq 2} n^kP_{\rm ch}(n) - 2^kP_{\rm el}\right]/(1-P_{\rm el}), \tag{20}$$

where $P_{\rm el}$ is the probability of elastic scattering.

It is now necessary to discuss the determination of the fireball mass m_F^*. The colliding quark in one of the incident hadrons has probability $f^c(x)$ of carrying a fraction x of that hadron's c.m. momentum p and the initial momentum of that colliding constituent quark is therefore xp. After the collision, the total momentum of the system of particles associated with the colliding constituent quark is $xp-\Delta$, where Δ is the impulse. In calculations at finite momentum, Δ is not allowed to exceed the largest of the c.m. momenta of the two colliding constituent quarks. If the colliding constituent quark generates a secondary-hadron fireball, the spectator quarks pick up a bare quark from the system of quarks generated from the colliding constituent quark to create a leading outgoing hadron. The probability that the bare quark picked up to form the leading hadron carries a fraction y of the momentum of the system of quarks generated from the colliding constituent quark was assumed to be given by $g_k(y)$, where k is the number of gluons which accompanied the valence quark prior to the collision *or* the number of gluons emitted by an unaccompanied valence quark during the collision. Consequently, the total momentum of the secondary-hadron fireball generated by the colliding constituent quark considered above is

$$p_F = (1-y)(xp-\Delta)\ , \tag{21}$$

while the momentum of the leading hadron is

$$p_L = (1-x)p + y(xp-\Delta)\ . \tag{22}$$

In the case where final-state hadrons are assumed to be either nucleons or pions, the invariant mass of the secondary-hadron fireballs created in inelastic-scattering events can now be calculated from kinematics. In events where only one secondary-hadron fireball is created in nucleon-nucleon scattering, the invariant fireball mass m_F^* is determined from

$$E_{\rm c.m.} = [(p-\Delta)^2 + m_N^{\,2}]^{1/2} + (p_L^{\,2} + m_N^{\,2})^{1/2} + (p_F^{\,2} + m_F^{*2})^{1/2}\ , \tag{23}$$

where $E_{\rm c.m.}$ is the c.m. energy, m_N is the nucleon mass, and p_L and p_F are given by Eqs. (21) and (22). In finite-momentum calculations, if $m_F^* < m_\pi$ for a particular combination of k, x_B, y_B, x_T, and y_T in Eq. (18), secondary-hadron production is not energetically possible and the associated probability is added as a contribution to the elastic-scattering probability.

In the case where two secondary-hadron fireballs are created, the mass of each fireball is obtained from

$$(p^2 + m_N^{\,2})^{1/2} = (p_L^{\,2} + m_N^{\,2})^{1/2} + (p_F^{\,2} + m_F^{*2})^{1/2}\ , \tag{24}$$

where p_L and p_F for the beam (target) systems determine the mass m_F^* of the hadron fireball associated with the beam (target) system.

Equation (24) assumes that the four-momentum transfer between the scattering systems is the minimum compatible with three-momentum transfer Δ (or the largest of the c.m. momenta of the colliding constituent quarks, if this is less than Δ) and involves no energy transfer. If m_F^* for one of the fireballs is less than m_π, the mass of that fireball is set equal to m_π and the mass of the remaining fireball is calculated from energy conservation. If, for given values of k, l, x_B, y_B, x_T, y_T in Eq. (18), both fireballs have an invariant mass less than m_π, secondary-hadron production is not possible and the associated probability is added as a contribution to the elastic-scattering probability.

GENERAL RESULTS

Three results are built into the model.

(i) The average transverse momentum of secondary hadrons [transverse to the jet (beam) direction] is constant. Note that the average transverse momentum is different for fireballs of different multiplicity, just as in my earlier model for e^+e^- annihilation.[1] It is only the transverse momentum averaged over all fireball multiplicities which is constant. The value chosen for the average transverse momentum of secondary hadrons is 360 MeV/c.

(ii) The longitudinal momentum transfer is negligible in high-energy hadronic-scattering reactions. In this model, the force between two colliding hadrons is an impulsive force in the c.m. system, so the c.m. momentum p' of the beam and target hadronic systems after an inelastic collision is related to the initial c.m. momentum by $p' = p - \Delta$. Since Δ was chosen as

1.8 GeV/c, $p' \approx p$ at high energies, and the model approximately satisfies the minimal rule of Benecke, Chou, Yang, and Yen[16] which states that only infinitesimal longitudinal momentum transfer is allowed at asymptotic energies.

(iii) The ratio of elastic to total cross section σ_{el}/σ_{tot} becomes constant at high energies. In proton-proton scattering, the experimental ratio σ_{el}/σ_{tot} is approximately 0.175 for all incident laboratory proton momenta above about 100 GeV/c. This ratio is constant at high energy in my model since μ_h in Eq. (2) was chosen as 0.436.

The following general results are also obtained from the model.

(a) Since the three-momentum transfer Δ is constant, the average charged multiplicity grows as $E^{1/4}$ at asymptotic energies, where E is the incident laboratory nucleon beam energy. The constant value of the three-momentum transfer Δ in the c.m. frame for high-energy hadronic scattering implies [through Eqs. (23) and (24)] that the average invariant mass of the secondary-hadronic fireballs produced in inelastic collisions rises as $E^{1/4}$. Then the assumption, implicit in Eq. (6), that the average number of secondary hadrons is a linear function of the invariant mass of the fireball leads to an average charged-hadron multiplicity growing as $E^{1/4}$ at asymptotic energies. In fact, there are indications[17] from cosmic-ray experiments that the average charged multiplicity grows faster above about 5 TeV in the lab (approximately 100 GeV in the c.m.) than would be indicated by the $a+b\ln s$ form commonly used[18] at lower energies.

(b) The fraction of scattering events of different types is constant at high energies. Since μ_n is chosen as 0.436 to obtain $\sigma_{el}/\sigma_{tot}=0.175$ at high energies, Eq. (11) states that in $P_Q(0)=64.7\%$ of events, the colliding constituent quark in one of the incident nucleons consists of a valence quark unaccompanied by virtual gluons, while in the remaining $1-P_Q(0)=35.3\%$ of events, the colliding constituent quark contains virtual gluons which are the precursors of a hadronic fireball. Similarly, Eq. (13) says that the probability of a colliding constituent quark producing no secondary hadronic fireball is $P_Q^2(0)=41.8\%$, while the probability that the quark creates a fireball from gluons emitted during the collision or accompanying it prior to the collision is

$$[1+P_Q(0)]\sum_{k=1}^{\infty}P_Q(k)=58.2\%\,.$$

Finally, when the colliding quarks in each incident hadron are considered as in Eq. (14) the breakdown of events is as follows:

Elastic events $P_{QB}^2(0)P_{QT}^2(0)=17.5\%$,

Target-fireball events $P_{QB}^2(0)[1+P_{QT}(0)]\sum_{k=1}^{\infty}P_{QT}(k)=24.3\%$,

Beam-fireball events $P_{QT}^2(0)[1+P_{QB}(0)]\sum_{k=1}^{\infty}P_{QB}(k)=24.3\%$,

Two-fireball events $\left\{[1+P_{QB}(0)]\sum_{k=1}^{\infty}P_{QB}(k)\right\}\left\{[1+P_{QT}(0)]\sum_{k=1}^{\infty}P_{QT}(k)\right\}=33.9\%$.

(c) Based on the assumption that a gluon carries (on the average) twice as much momentum as a quark, the fraction of a proton's momentum carried by the electrically neutral gluons is, on the average, $2\mu_n/(1+2\mu_n)=46.6\%$. Correspondingly, the average percentage of the proton's momentum carried by charged matter (the quarks) is 53.4%, in agreement with the result extracted from experiment.[19]

NUMERICAL CALCULATIONS OF MULTIPLICITY DISTRIBUTIONS

To carry out explicit numerical calculations with Eq. (18), two numerical approximations are necessary. (1) The infinite sums over the number of gluons dressing a quark must be truncated. This is done by truncating the sums over $P_{QB}(i)$ and $P_{QT}(i)$ at some integer A and setting $P_Q(A)=1-\sum_{k=0}^{A-1}P_Q(k)$ to preserve the proper normalization (conserve probability). (2) The integrals over the constituent- and valence-quark momentum distributions must be approximated by finite sums.

The numerical integration

$$\int_0^1 f^c(x)dx=20\int_0^1 x(1-x)^3dx$$
$$=20\sum_{i=1}^{N}w^c(x_i)x_i(1-x_i)^3+R_N$$

uses Formula 25.4.33 of Abramowitz and Stegun,[20] with the abscissas x_i and the weights w_i provided in Table 25.8 of that reference. The remainder R_N is proportional to $f^{c(2N)}(\xi)$ for $0<\xi<1$. The fifth derivative of $f^c(x)$ is zero, so the remainder term is zero for numerical integration of order $N\geq 3$.

The numerical integration

$$\int_0^1 g_k(y)dy = A_k \int_0^1 \frac{(1-y)^{k-1}}{\sqrt{y}}\, dy$$

can be transformed by the variable change $y = 1 - t$ into

$$\int_0^1 g_k(y)dy = A_k \int_0^1 \frac{t^{k-1}}{(1-t)^{1/2}}\, dt .$$

The numerical integration then uses Formula 25.4.36 of Ref. 20 so

$$\int_0^1 g_k(y)dy = A_k \sum_{i=1}^{M} w_k(i)\, t_i^{k-1} + R_M .$$

The abscissas $t_i = 1 - \xi_i^2$, where ξ_i is the ith positive zero of $P_{2N}(x)$ (the Legendre polynomial of order $2N$) and the weights $w_k(i) = 2w_i^{2N}$, where w_i^{2N} are the Gaussian weights of order $2N$, are provided in Table 25.4 of Ref. 20. The remainder R_M is proportional to the $2M$th derivative of ξ^{k-1} with $0 < \xi < 1$. Since the kth derivative of ξ^{k-1} is zero, the remainder term R_M is zero for numerical integration of $g_k(y)$ when $k < 2M$. Therefore,

$$\int_0^1 g_k(y)dy = A_k \sum_{i=1}^{M} w_k(i)(1-\xi_i^2)^{k-1} + R_M .$$

When these numerical approximations are applied to Eq. (18), the equation which results is

$$\begin{aligned}
P'_{ch}(b) = {} & \delta_{b0} P_{QB}^2(0) P_{QT}^2(0) \\
& + 400 \sum_{i_B=1}^{N} \sum_{i_T=1}^{N} w^c(x_{i_B}) x_{i_B} (1-x_{i_B})^3 w^c(x_{i_T}) x_{i_T} (1-x_{i_T})^3 \\
& \times \Big\{ P_{QB}^2(0)[1+P_{QT}(0)] \sum_{k=1}^{A} P_{QT}(k) \sum_{j_T=1}^{M} A_k w_k(j_T)(1-\xi_{j_T}^2)^{k-1} P_c[b, m_F^*(k, x_{i_B}, x_{i_T}, \xi_{j_T}^2)] \\
& + P_{QT}^2(0)[1+P_{QB}(0)] \sum_{k=1}^{A} P_{QB}(k) \sum_{j_B=1}^{M} A_k w_k(j_B)(1-\xi_{j_B}^2)^{k-1} P_c[b, m_F^*(k, x_{i_T}, x_{i_B}, \xi_{j_B}^2)] \\
& + [1+P_{QB}(0)][1+P_{QT}(0)] \sum_{k=1}^{A} \sum_{l=1}^{A} A_k A_l P_{QB}(k) P_{QT}(l) \\
& \times \sum_{j_B=1}^{M} \sum_{j_T=1}^{M} w_k(j_B)(1-\xi_{j_B}^2)^{k-1} w_l(j_T)(1-\xi_{j_T}^2)^{l-1} \\
& \times \sum_{a=0}^{b} P_c[b-a, m_{BF}^*(k, x_{i_B}, \xi_{j_B}^2, x_{i_T}, \xi_{j_T}^2)] \\
& \times P_c[a, m_{TF}^*(l, x_{i_B}, \xi_{j_B}^2, x_{i_T}, \xi_{j_T}^2)] \Big\} . \qquad (25)
\end{aligned}$$

This is the explicit form used as the basis for all numerical calculations of multiplicity distributions in this paper. The remaining inputs needed are the following.

(a) The Poisson distributions $P_{QB}(k)$ and $P_{QT}(k)$ given by Eq. (2) with $\mu_h = 0.436$.

(b) $A_k = \Gamma(k+\frac{1}{2})/[\Gamma(\frac{1}{2})\Gamma(k)]$ from Eq. (10).

(c) The distribution function $P_c(b, m_F^*)$ given by Eq. (15). For large values of n, the truncated Poisson distribution $P_F(n)$ given in Eq. (5) which is used to calculate $P_c(b, m_F^*)$ can be approximated as

$$P_F(n) = \frac{\alpha}{(2\pi n)^{1/2}} \left(\frac{\xi}{n}\right)^n e^{n-\xi}$$

using Stirling's approximation.

First, a calculation of the charged-hadron multiplicity distribution in proton-proton scattering at a c.m. energy of 27.6 GeV was undertaken with the number of gluons considered truncated at $k = 3$. From Eq. (2), the probability that a quark is dressed by less than four gluons (when $\mu_n = 0.436$) is $\sum_{k=0}^{3} P_Q(k) = 0.9989$. Furthermore, the probability that a constituent quark containing gluons contains only one, two, or three gluons is $\sum_{k=1}^{3} P_Q(k)/[1-P_Q(0)] = 0.9970$. The results of this calculation (denoted calculation 0) were within a few percent of those obtained from the considerably faster version of the model to be discussed next. Because the initial calculation used too much computer time, it was necessary to consider a series of physical approximations which also lead to numerical simplifications. These approximations show that the desirable features of the numerical results are not easily destroyed by simplifying approximations. Therefore, to explore the characteristics of the model with the limited financial resources available, all subsequent calculations were based on the simpler versions of the model discussed below.

Calculation 1. In this calculation, a valence quark is assumed to be dressed by either zero

gluons or one gluon and conservation of probability is ensured by taking $P_Q(1)=1-P_Q(0)$. This approximation is pretty good because the probability (when $\mu_n=0.436$) that a constituent quark consists of a valence quark dressed by zero gluons or one gluon is $P_Q(0)+P_Q(1)=0.9825$ and the probability that a constituent quark containing gluons contains only one gluon is $P_Q(1)/[1-P_Q(0)]=0.7978$. This model is obtained from Eq. (25) by setting $k=l=1$, removing the sums over those indices and setting $P_Q(1)=1-P_Q(0)$.

Calculation 2. This calculation considers only the distribution of constituent quark momenta within the colliding nucleons. It is assumed that, in any event where secondary hadrons are produced, the quark picked up by the spectators to form the leading hadron always carries exactly $\frac{1}{3}$ of the momentum of the scattered constituent quark. That is, in addition to assuming that the valence quarks are dressed by zero gluons or one gluon, as in calculation 1, it is assumed that the fragments of a scattered constituent quark always share the momentum of that quark equally. This model is obtained from Eq. (18) by first setting $k=l=1$, removing the sums over those indices and setting $P_Q(1)=1-P_Q(0)$. Next, $g_k(y)$ is defined as $g_k(y)=\delta_{k1}\delta(y-\frac{1}{3})$ so the numerical integration over the y variable disappears.

Calculation 3. This is the simplest version of the model, similar in concept to the model I outlined previously in Ref. 4. In this calculation, the distribution of constituent quark momenta within the colliding hadrons and the distribution of valence quark momenta within the constituent quarks are both neglected. Thus, it is assumed that (i) valence quarks are dressed by either zero or one gluon, (ii) when a constituent quark breaks up to form secondary hadrons, the quark picked up by the spectators to form the leading hadron always carries exactly $\frac{1}{3}$ of the momentum of the scattered constituent quark, and (iii) the incident constituent quark always carries exactly $\frac{1}{3}$ of the momentum of the colliding hadron. The last assumption is the one which differentiates this calculation from calculation 2.

This version of the model is obtained from Eq. (18) by (a) setting $k=l=1$, removing the sums over these indices and setting $P_Q(1)=1-P_Q(0)$, (b) defining $g_k(y)=\delta_{k1}\delta(y-\frac{1}{3})$ so the numerical integrations over the y variables drop out, and (c) defining $f^c(x)=\delta(x-\frac{1}{3})$ so the numerical integrations over the x variables drop out. In the notation of Eq. (18), the resulting equation used in calculation 3 can be written

$$P'_{\rm ch}(b)=\delta_{b0}P_{QB}{}^2(0)P_{QT}{}^2(0)+\{P_{QB}{}^2(0)[1-P_{QT}{}^2(0)]+P_{QT}{}^2(0)[1-P_{QB}{}^2(0)]\}P_c[b,m_F^*(1,\tfrac{1}{3},\tfrac{1}{3},\tfrac{1}{3})]$$
$$+[1-P_{QB}{}^2(0)][1-P_{QT}{}^2(0)]\sum_{a=0}^{\infty}P_c[b-a,m_F^*(1,\tfrac{1}{3},\tfrac{1}{3},\tfrac{1}{3},\tfrac{1}{3})]P_c[a,m_F^*(1,\tfrac{1}{3},\tfrac{1}{3},\tfrac{1}{3},\tfrac{1}{3})]. \quad (26)$$

This version possesses the same general characteristics as the more complex versions and reproduces the general features of the charged-hadron multiplicity distributions. However, it will obviously lead to an unrealistic description of the longitudinal-momentum distribution of final-state hadrons because the leading hadron associated with a secondary-hadronic fireball in this version of the model always carries exactly $\frac{7}{9}$ of the momentum of the scattered system.

In addition to the above calculations, two numerical estimates of the average charged-hadron multiplicity in proton-proton scattering were obtained. In these calculations, the estimated charged-hadron multiplicity was determined without calculating the multiplicity distributions. These calculations were based on the following numerical approximation for the average charged-hadron multiplicity in proton-proton scattering:

$$\langle n_{\rm ch}\rangle \approx 2+400\sum_{i_B=1}^{N}\sum_{i_T=1}^{N} w^c(x_{i_B})x_{i_B}(1-x_{i_B})^3 w^c(x_{i_T})x_{i_T}(1-x_{i_T})^3$$
$$\times\Bigg\{P_{QB}{}^2(0)[1+P_{QT}(0)]\sum_{k=1}^{A}P_{QT}(k)\sum_{j_T=1}^{M}A_k w_k(j_T)(1-\xi_{j_T}{}^2)^{k-1}(\tfrac{2}{3})\frac{m_F^*}{(p_H{}^2+m_\pi{}^2)^{1/2}}$$
$$+P_{QT}{}^2(0)[1+P_{QB}(0)]\sum_{k=1}^{A}P_{QB}(k)\sum_{j_B=1}^{M}A_k w_k(j_B)(1-\xi_{j_B}{}^2)^{k-1}(\tfrac{2}{3})\frac{m_F^*}{(p_H{}^2+m_\pi{}^2)^{1/2}}$$
$$+[1+P_{QB}(0)][1+P_{QT}(0)]\sum_{k=1}^{A}\sum_{l=1}^{A}P_{QB}(k)P_{QT}(l)$$
$$\times\sum_{j_B=1}^{m}\sum_{j_T=1}^{m}A_kA_l w_k(j_B)(1-\xi_{j_B}{}^2)^{k-1}w_l(j_T)(1-\xi_{j_T}{}^2)^{l-1}$$
$$\times[\tfrac{2}{3}m_{BF}^*/(p_H{}^2+m_\pi{}^2)^{1/2}+\tfrac{2}{3}m_{TF}^*/(p_H{}^2+m_\pi{}^2)^{1/2}]\Bigg\}. \quad (27)$$

The first term in this equation arises from charge conservation, since there are two charged hadrons (protons) in the initial state. The remaining three terms, which give an approximation to the weighted average number of secondary hadrons (pions) produced by the fireballs were obtained from the analogous terms of Eq. (25) as follows: (1) Replace the distribution P_c in the first two terms in the bracket in Eq. (25) by

$$\tfrac{2}{3} m_F^*/(p_H{}^2 + m_\pi{}^2)^{1/2}.$$

(2) Replace the convolution in the last term in the bracket in Eq. (25) by

$$\{[\tfrac{2}{3} m_{BF}^*/(p_H{}^2 + m_\pi{}^2)^{1/2}] + [\tfrac{2}{3} m_{TF}^*/(p_H{}^2 + m_\pi{}^2)^{1/2}]\}.$$

This assumes that the distribution P_c can be approximated by a Poisson distribution, the truncation of the P_c distribution can be neglected, and the mean of the distribution P_c can be approximated by

$$\tfrac{2}{3} m_F^*/(p_H{}^2 + m_\pi{}^2)^{1/2}$$

since all of the secondary hadrons have been assumed to be pions and the mean number of secondary hadrons in a fireball is $m_F^*/(p_H{}^2 + m_\pi{}^2)^{1/2}$. The fact that the mean of a convolution of Poisson distributions is the sum of the means of the convoluted distributions has also been used in developing Eq. (27).

Two calculations were carried out based on Eq. (27).

Calculation A. This calculation is analogous to calculation 0 discussed previously. In this calculation, constitutent quarks are assumed to contain zero, one, two, or three gluons (i.e., $A = 3$).

Calculation B. This calculation is analogous to the previously discussed calculation 1. Valence quarks are assumed to be dressed by either zero gluons or one gluon and conservation of probability is ensured by setting $P_Q(1) = 1 - P_Q(0)$ (i.e., $A = 1$).

Five-point integration formulas ($M = N = 5$) were used for all numerical integrations over internal momentum distributions. Three-point integration formulas are somewhat faster, and give results within a few percent of the five-point formulas at c.m. energies above about 10 GeV. However, at low energies, the mass of the secondary hadronic fireball can be less than m_π for some values of the fraction x of the hadron momentum carried by the scattered constituent quark and the fraction y of the momentum of the scattered constituent quark which is carried by the constituent-quark-fragment picked up by the spectators to form the leading hadron. In this model, the probability of energetically inaccessible production events (i.e., the probability of events with fireball mass less than m_π) is added into the probability of elastic scattering. Because the five-point numerical integration samples more points on the internal-momentum distribution spectra, it provides a smoother representation of the variation of the percentage of elastic scattering at low energy.

Table I compares the results of calculations 0, 1, 2, and 3 for proton-proton scattering at a c.m. energy of 27.6 GeV with the experimental values taken from Dado *et al.*[21] The results of calculations 0 and 1 lie within 1% of each other except for the parameter f_2. The calculation was also performed with three- and six-point numerical integrations, and the results were within a few percent of the results tabulated in Table I, except for the parameter f_2 which varied as much as 20%.

Table II presents information on the average charged-hadron multiplicity $\langle n \rangle$ in inelastic proton-proton scattering and the percentage of elastic-scattering events for c.m. energies from 3 to 300 GeV. The experimental values for $\langle n \rangle$ at c.m. energies from 13.8 to 62.8 GeV were taken from

TABLE I. Experimental and calculated values of charged-hadron multiplicity distribution parameters for proton-proton scattering at a c.m. energy of 27.6 GeV. Experimental data from Dado *et al.* (Ref. 21), except D_3 and D_4, which are obtained from the fits to experimental data provided by Thome *et al.* (Ref. 22). All calculations give the percentage of elastic scattering as 17.5%, and use five-point numerical integrations for the internal-momentum distributions.

Parameter	Experimental value	Calculation 0	Calculation 1	Calculation 2	Calculation 3
$\langle n \rangle$	8.83	9.25	9.16	9.26	9.62
$D_2 = [\langle (n - \langle n \rangle)^2 \rangle]^{1/2}$	4.59	3.82	3.78	3.67	3.23
$D_3 = [\langle (n - \langle n \rangle)^3 \rangle]^{1/3}$	4.09	3.12	3.10	2.86	2.25
$D_4 = [\langle (n - \langle n \rangle)^4 \rangle]^{1/4}$	6.20	5.16	5.11	4.91	4.28
$f_2 = \langle n(n-1) \rangle - \langle n \rangle^2$	12.2	5.37	5.16	4.20	0.82
$\langle n^2 \rangle / \langle n \rangle^2$	1.25	1.17	1.17	1.16	1.11
$\langle n^3 \rangle / \langle n \rangle^3$	1.84	1.55	1.55	1.50	1.35
$\langle n^4 \rangle / \langle n \rangle^4$	3.05	2.28	2.28	2.14	1.77

TABLE II. Average charged-hadron multiplicities and percentage of elastic scattering. The first two rows show the experimental value of the average charged-hadron multiplicity and the source of the charged-hadron multiplicity data: Dado *et al.* (Ref. 21) or Thome *et al.* (Ref. 22). The third row shows the value of the charged-hadron multiplicity predicted by the Albini *et al.* parametrization (Ref. 18) $\langle n\rangle_{\text{Albini}} = 2.5 + 0.28 \ln (E - 2m_N) + 0.53 [\ln (E - 2m_N)]^2$. The subsequent rows show the average charged-hadron multiplicities in inelastic-scattering events and the percentage of elastic scattering for the calculations discussed in the text.

c.m. energy (GeV)	3.0	5.0	10.0	13.8	19.7	23.6	27.6	30.8	45.2	53.2	62.8	150.0	300.0
$\langle n\rangle$ (experiment)				6.39	7.67	8.12	8.83	9.54	11.01	11.77	12.70		
Data source (Ref. No.)				21	21	22	21	22	22	22	22		
$\langle n\rangle$ (Albini *et al.*[18])	2.54	3.51	5.41	6.45	7.70	8.38	9.00	9.44	11.08	11.82	12.60	17.14	21.30
Calculation 1													
$\langle n\rangle$	2.26	3.56	5.81	6.85	8.01	8.60	9.16	9.57	11.22	12.02	12.89	18.87	25.90
% elastic	23.3	18.6	17.5	17.5	17.5	17.5	17.5	17.5	17.5	17.5	17.5	17.5	17.5
Calculation 2													
$\langle n\rangle$	2.25	3.54	5.85	6.89	8.06	8.67	9.26	9.70	11.40	12.23	13.14	19.39	26.72
% elastic	21.5	17.8	17.5	17.5	17.5	17.5	17.5	17.5	17.5	17.5	17.5	17.5	17.5
Calculation 3													
$\langle n\rangle$	2.15	3.43	6.14	7.27	8.38	9.02	9.62	10.06	11.82	12.68	13.63	20.14	27.79
% elastic	17.5	17.5	17.5	17.5	17.5	17.5	17.5	17.5	17.5	17.5	17.5	17.5	17.5
Calculation A													
$\langle n\rangle$	2.56	3.70	5.86	6.91	8.09	8.71	9.28	9.72	11.43	12.25	13.16	19.32	26.55
% elastic	23.8	18.7	17.5	17.5	17.5	17.5	17.5	17.5	17.5	17.5	17.5	17.5	17.5
Calculation B													
$\langle n\rangle$	2.47	3.71	5.86	6.90	8.05	8.64	9.19	9.61	11.27	12.07	12.94	18.92	25.95
% elastic	23.3	18.6	17.5	17.5	17.5	17.5	17.5	17.5	17.5	17.5	17.5	17.5	17.5

Dado *et al.*[21] and Thome *et al.*[22] The experimental values of the charged-hadron multiplicity are compared to the calculated values and to the Albini *et al.* parametrization[18] $\langle n\rangle_{\text{Albini}} = 2.5 + 0.28 \ln(E - 2m_n) + 0.53[\ln(E - 2m_n)]^2$ which can be used to represent the experimental data on average charged multiplicities in pp collisions at c.m. energies below 150 GeV.

Calculation 1 gives multiplicities between 1% and 7% higher than the experimental values over the energy range 13.8 to 62.8 GeV, while the Albini *et al.* parametrization gives multiplicities which vary from 1% below to 4% above the experimental multiplicities in the same range.

Calculation 1 gives a multiplicity which is 11% lower than the Albini *et al.* value at 3 GeV. The multiplicities from calculation 1 are higher than the Albini *et al.* values at all other tabulated energies, but they lie within 10% of the Albini values at energies up to 150 GeV.

Since the average charged multiplicity in this model grows as $E^{1/4}$, all calculations predict substantially higher charged multiplicities above 150 GeV than would be predicted by the Albini *et al.* parametrization if it is extended above 150 GeV, outside its range of applicability. This is in agreement with the trend observed in cosmic-ray data.[17]

Calculation 2 gives multiplicities varying between 1% below those predicted by calculation 1 at low energies to 4% above the calculation 1 values at the highest energies tabulated.

The multiplicites obtained from calculation 3 vary from 5% below the calculation 1 values at low energies to 8% above the calculation 1 value at the highest energy tabulated. Calculation 3, which is the simplest form of the model, predicts multiplicities between 6% and 14% higher than the experimental values over the energy range 13.8 to 62.8 GeV.

Turning to the approximate calculations of the average charged multiplicity based on Eq. (27), it is seen that the charged multiplicities obtained from calculation A lie within 3% of the values obtained from calculation B over the entire energy range 3 to 300 GeV. Calculation B is analogous to calculation 1 in that they both involve the approximation that valence quarks are dressed by either zero or one gluon. The value of the average charged multiplicity obtained from calculation B is 9% higher than the multiplicity obtained from calculation 1 at 3 GeV. This is to be anticipated, because the approximations used in developing Eq. (27) neglect the truncation of the fireball-decay multiplicity distribution required by energy conservation. At higher energies, the effects of

neglecting the truncation become less significant, and the results of calculation B approach those of calculation 1 until they differ by less than 1% at 300 GeV.

Table III provides information on the moments of the multiplicity distribution $D_q = [\langle (n - \langle n \rangle)^q \rangle]^{1/q}$. The experimental values of D_2 are taken from the same sources as the average-charged-multiplicity data in Table II. The rows labeled D_q^{fit} are calculated from the following fits to experimental data presented by Thome *et al.*[22]:

$$D_2 = 0.576(\langle n \rangle - 0.968),$$

$$D_3 = 0.522(\langle n \rangle - 0.995),$$

$$D_4 = 0.799(\langle n \rangle - 1.067).$$

The calculated values of D_q show the same qualitative behavior between 13.8 and 62.8 GeV in the c.m. as the experimental results, rising as an approximately linear function of $\langle n \rangle$. However, the calculated values of D_q are progressively smaller at any given energy as one proceeds from calculation 1 to calculation 3. This indicates that the calculated multiplicity distributions are narrower than the experimentally observed distributions. It also shows that more realistic treatment of the internal-momentum distributions within the colliding hadrons tends to broaden the multiplicity distributions, as expected. The calculated values of D_q rise more slowly as a function of energy than the experimental values, and the values obtained from calculation 3 rise the slowest of all.

The calculated values of the correlation function $f_2 = \langle n(n-1) \rangle - \langle n \rangle^2$ and the first three reduced moments $\langle n^q \rangle / \langle n \rangle^q$ of the charged-hadron multiplicity distribution in proton-proton scattering are compared to experimental data in Table IV. The experimental values are taken from the same sources as in Table II. The calculated values of the correlation function f_2 show the same general behavior as the experimental values, but they rise slower with increasing c.m. energy. Above about 5 GeV in the c.m. the calculated values of the reduced moments fall very slowly as the energy increases, instead of rising slowly as suggested by the experimental data accumulated between 13.8 and 62.8 GeV.

At very high energies, where the number of secondary hadrons which can be produced becomes very large, the numerical formulation of this model should be modified to facilitate calculations. This might be done, for example, by approximating the truncated Poisson distributions by normal distributions and replacing the discrete sums over secondary-hadron multiplicities with integrals. In the absence of experimental data with which to make detailed comparisons, this is not a particularly pressing task. However, in anticipation of future generations of particle accelerators,[23] it is interesting to attempt a prediction of the charged-hadron multiplicities at very high energies. The easiest way to do this is to employ the (approximate) calculations A and B, which have been shown to give results in close agreement to those provided by the more detailed calculations at c.m. energies above about 10 GeV. Consequently, calculations A and B were performed at c.m. energies of 500, 800, and 2000

TABLE III. The moments of the charged-hadron multiplicity distribution, $D_q = [\langle (n - \langle n \rangle)^q \rangle]^{1/q}$. Data sources for D_2 (experiment) are the same as in Table II for the corresponding c.m. energy. D_q (Thome *et al.* fit) are the fits to experimental data presented by Thome *et al.* (Ref. 22): $D_2 = 0.576(\langle n \rangle - 0.968)$, $D_3 = 0.522(\langle n \rangle - 0.995)$, and $D_4 = 0.799(\langle n \rangle - 1.067)$.

c.m. energy (GeV)	3.0	5.0	10.0	13.8	19.7	23.6	27.6	30.8	45.2	53.2	62.8	150.0	300.0
$D_2 = [\langle (n - \langle n \rangle)^2 \rangle]^{1/2}$													
Experiment				3.21	3.82	4.05	4.59	4.83	5.90	6.39	6.92		
Thome *et al.* fit (Ref. 22)				3.12	3.86	4.12	4.53	4.94	5.78	6.22	6.76		
Calculation 1	0.71	1.75	2.66	2.94	3.33	3.56	3.78	3.95	4.62	4.95	5.31	7.83	10.76
Calculation 2	0.70	1.72	2.62	2.90	3.26	3.48	3.67	3.81	4.39	4.67	4.98	7.05	9.42
Calculation 3	0.53	1.43	2.32	2.62	2.91	3.08	3.23	3.34	3.78	3.99	4.21	5.66	7.22
$D_3 = [\langle (n - \langle n \rangle)^3 \rangle]^{1/3}$													
Thome *et al.* fit (Ref. 22)				2.82	3.48	3.72	4.09	4.46	5.23	5.62	6.11		
Calculation 1	0.98	1.79	2.27	2.39	2.68	2.90	3.10	3.25	3.82	4.08	4.36	6.06	7.75
Calculation 2	0.97	1.76	2.24	2.34	2.56	2.72	2.86	2.97	3.38	3.58	3.78	5.01	6.20
Calculation 3	0.79	1.27	1.72	1.87	2.04	2.14	2.25	2.33	2.64	2.79	2.95	3.98	5.09
$D_4 = [\langle (n - \langle n \rangle)^4 \rangle]^{1/4}$													
Thome *et al.* fit (Ref. 22)				4.25	5.28	5.64	6.20	6.77	7.94	8.55	9.29		
Calculation 1	1.25	2.47	3.58	3.95	4.49	4.81	5.11	5.34	6.22	6.65	7.13	10.33	14.03
Calculation 2	1.23	2.44	3.54	3.89	4.37	4.66	4.91	5.10	5.86	6.23	6.63	9.31	12.36
Calculation 3	0.99	1.89	3.08	3.47	3.86	4.08	4.28	4.44	5.02	5.30	5.59	7.47	9.45

TABLE IV. Correlation function and reduced moments for charged-hadron multiplicity distributions. The data sources for the correlation function $f_2 = \langle n(n-1)\rangle - \langle n\rangle^2$ and the reduced moments $\langle n^q\rangle/\langle n\rangle^q$ are the same as for the corresponding c.m. energies in Table II.

c.m. energy (GeV)	3.0	5.0	10.0	13.8	19.7	23.6	27.6	30.8	45.2	53.2	62.8	150.0	300.00
$f_2 = \langle n(n-1)\rangle - \langle n\rangle^2$													
Experiment				3.9	6.9	8.3	12.2	13.76	23.78	29.10	35.20		
Calculation 1	−1.76	−0.51	1.26	1.81	3.09	4.09	5.16	6.04	10.09	12.44	15.33	42.50	89.81
Calculation 2	−1.76	−0.59	1.03	1.52	2.59	3.44	4.20	4.85	7.89	9.60	11.65	30.34	61.99
Calculation 3	−1.87	−1.39	−0.74	−0.40	0.09	0.45	0.82	1.12	2.48	3.23	4.13	11.85	24.32
$\langle n^2\rangle/\langle n\rangle^2$													
Experiment				1.25	1.25	1.25	1.25	1.26	1.29	1.30	1.30		
Calculation 1	1.10	1.24	1.21	1.18	1.17	1.17	1.17	1.17	1.17	1.17	1.17	1.17	1.17
Calculation 2	1.10	1.24	1.20	1.18	1.16	1.16	1.16	1.15	1.15	1.15	1.14	1.13	1.12
Calculation 3	1.06	1.17	1.14	1.13	1.12	1.12	1.11	1.11	1.10	1.10	1.10	1.08	1.07
$\langle n^3\rangle/\langle n\rangle^3$													
Experiment				1.84	1.84	1.84	1.84	1.86	1.99	2.01	2.02		
Calculation 1	1.38	1.85	1.69	1.60	1.56	1.55	1.55	1.55	1.55	1.55	1.55	1.55	1.54
Calculation 2	1.37	1.83	1.66	1.57	1.52	1.51	1.50	1.49	1.47	1.46	1.45	1.41	1.39
Calculation 3	1.23	1.57	1.45	1.41	1.38	1.36	1.35	1.34	1.32	1.31	1.30	1.24	1.21
$\langle n^4\rangle/\langle n\rangle^4$													
Experiment				3.05	3.05	3.05	3.05	3.12	3.53	3.58	3.60		
Calculation 1	2.01	3.19	2.64	2.39	2.29	2.28	2.28	2.28	2.27	2.27	2.27	2.26	2.23
Calculation 2	1.99	3.13	2.57	2.32	2.20	2.17	2.14	2.12	2.07	2.04	2.02	1.92	1.84
Calculation 3	1.61	2.33	2.01	1.90	1.83	1.79	1.77	1.75	1.69	1.67	1.64	1.52	1.44

GeV, and the resulting estimates of the average charged-hadron multiplicities are shown in Table V. These energies were chosen because they lie near the tops of the operating ranges of the following proposed accelerators which were listed in Ref. 23: the SPS $p\bar{p}$ machine at CERN with a maximum c.m. energy of 540 GeV, the ISABELLE pp machine at Brookhaven with a maximum c.m. energy of 800 GeV, and the Fermilab $p\bar{p}$ machine with a maximum c.m. energy of 2000 GeV. The applicability of the 500 and 2000 GeV estimates in Table V depend, of course, on the assumptions that annihilation events are a decreasing proportion of $p\bar{p}$ scattering events at very high energies and that pp and (nonannihilation) $p\bar{p}$ scattering events are essentially identical at very high energies.

CALCULATION OF LONGITUDINAL RAPIDITY DISTRIBUTIONS

The longitudinal rapidity distribution of charged final-state hadrons is often measured in scattering experiments. The longitudinal rapidity distribution of charged pions generated by the model described above can be calculated using an approach similar to that employed in my paper on e^+e^- annihilation.[1]

In this model for hadronic scattering, secondary hadrons are produced by isotropic decay (in the fireball rest frame) of fireballs with invariant mass m_F^*. The decay multiplicity of the fireballs is given by the truncated Poisson distribution (5). The fireball momentum p_F is given by Eq. (21) and depends on the fraction x of the incident hadron's momentum carried by the colliding constituent quark and the fraction y of the momentum of the scattered constituent quark which is carried by the bare quark picked up to form the leading hadron after the collision. The invariant mass m_F^* of the fireball is obtained from Eq. (23) or (24) depending on whether one or two fireballs is created in the scattering event. Therefore, in the overall c.m. frame for the hadronic scattering event, the fireball has

TABLE V. Estimates of average charged-hadron multiplicities in very-high-energy inelastic-scattering events.

c. m. energy (GeV)	500	800	2000
Average charged-hadron multiplicity			
Calculation A	33.74	42.21	65.74
Calculation B	32.95	41.20	64.10

$\vec{\beta}_F = \vec{p}_F/(p_F^2+m_F^{*2})^{1/2}$ and $\gamma_F = (p_F^2+m_F^{*2})^{1/2}/m_F^*$.

For fireball decays with multiplicity k, the energy of the decay products in the fireball rest frame is $E_k' = m_F^*/k$ and the fireball decay spectrum in the fireball-rest-frame momentum space forms a spherical shell with radius $|\vec{p}_k'| = (E_k'^2 - m_\pi^2)^{1/2}$, assuming that all decay products are pions.

When this spherical decay spectrum in the fireball-rest-frame momentum space is transformed into the overall-c.m. momentum space for the nucleon-nucleon scattering process, an analysis like that explained by Hagedorn[24] shows that the secondary pions from an event with fireball-decay multiplicity k lie on an ellipsoidal shell in the overall-c.m. momentum space with longitudinal c.m. momentum lying between

$$p_{k+} = \gamma_F(p_k' + \beta_F E_k')$$
and
$$p_{k-} = \gamma_F(-p_k' + \beta_F E_k'). \tag{28}$$

It can also be shown that the probability of finding a pion from a fireball with decay multiplicity k at any value of the c.m. longitudinal momentum between p_{k+} and p_{k-} is constant. Consequently, the occupation probability of a momentum interval Δp lying between p_{k+} and p_{k-} for secondary pions from a fireball decaying with multiplicity k is $k\Delta p/2\gamma_F p_k'$.

The longitudinal rapidity of a secondary hadron with longitudinal momentum p_l and energy E_s in the overall-c.m. system is defined as

$$y = \tfrac{1}{2}\ln\left(\frac{E_s+p_l}{E_s-p_l}\right).$$

The rapidity of secondary pions produced in a hadronic collision at c.m. energy E must lie between $\pm\frac{1}{2}Y$, where $Y = \ln(E/m_\pi)$. The longitudinal rapidity distribution of final-state hadrons then gives the average number of final-state hadrons observed at any given value of y.

The longitudinal rapidity distribution of charged final-state hadrons in my model for nucleon-nucleon scattering was then calculated as follows. The rapidity interval $(+\frac{1}{2}Y, -\frac{1}{2}Y)$ in the overall hadronic c.m. frame was divided into 40 bins for the computation, and only the final-state hadrons from inelastic-scattering events were considered. The longitudinal rapidity distribution of the final-state hadrons in inelastic-scattering events was calculated using a modification to Eq. (25) that is similar in nature to calculation 1 in the preceding section. It was assumed that a constituent quark is dressed by zero or one gluon, so the sums over k and l disappear and $P_Q(1)$ is taken equal to $[1-P_Q(0)]$. Furthermore, the P_c distributions in the last term are not convoluted. The resulting equation is

$$\begin{aligned}
1 = {} & P_{QB}^2(0)P_{QT}^2(0) \\
& + 400\sum_{i_B=1}^{N}\sum_{i_T=1}^{N} w^c(x_{i_B})x_{i_B}(1-x_{i_B})^3 w^c(x_{i_T})x_{i_T}(1-x_{i_T})^3 \\
& \times\Bigg\{P_{QB}^2(0)[1-P_{QT}^2(0)]\sum_{j_T=1}^{M} A_1 w_1(j_T)\sum_{n=0}^{n_{\max}/2} P_c[n, m_F^*(1, x_{i_B}, x_{i_T}, \xi_{j_T}^2)] \\
& + P_{QT}^2(0)[1-P_{QB}^2(0)]\sum_{j_B=1}^{M} A_1 w_1(j_B)\sum_{n=0}^{n_{\max}/2} P_c[n, m_F^*(1, x_{i_T}, x_{i_B}, \xi_{j_B}^2)] \\
& + [1-P_{QT}^2(0)][1-P_{QB}^2(0)]\sum_{j_B=1}^{M}\sum_{j_T=1}^{M} A_1^2 w_1(j_B)w_1(j_T) \\
& \qquad \times\sum_{n=0}^{n_{\max}/2} P_c[n, m_{BF}^*(1, x_{i_B}, \xi_{j_B}^2, x_{i_T}, \xi_{j_T}^2)] \\
& \qquad \times\sum_{n'=0}^{n_{\max}/2} P_c[n', m_{TF}^*(1, x_{i_B}, \xi_{j_B}^2, x_{i_T}, \xi_{j_T}^2)]\Bigg\}.
\end{aligned} \tag{29}$$

The longitudinal rapidity distribution of final-state hadrons in inelastic-scattering events receives contributions from each of the three bracketed terms of Eq. (29), since the first term corresponds to elastic scattering. Each of the terms in the curly bracket in Eq. (29) corresponds to a different possible outcome of an inelastic-scattering event with different values of the fireball momenta, the leading-hadron momenta, and the fireball multiplicity for decay into charged hadrons. Taking the first term in the bracket as an example, the probability

$$P_\alpha(x_{iB}, x_{iT}, \xi_{jT}^2) = 400 w^c(x_{iB})x_{iB}(1-x_{iB})^3 w^c(x_{iT})x_{iT}(1-x_{iT})^3 P_{QB}^2(0)[1-P_{QT}^2(0)]A_1 w_1(j_T)$$

of the occurrence of a one-fireball event with specific values of x_{i_B}, x_{i_T}, and $y_{j_T} = \xi_{j_T}{}^2$ is determined. Then, the value of the fireball momentum is determined, as are $\vec{\beta}_F$, γ_F, and the fireball mass m_F^*. Calculating the rapidity distribution of the charged pions is slightly complicated by the fact that fireball decays into final states with n charged-pion pairs receive contributions from fireballs with total decay multiplicity between $2n$ and m_F^*/m_π, the maximum decay multiplicity energetically allowed for the fireball. Consequently, Eq. (15) is used to relate the probability of $2n$ charged pions resulting from a fireball decay to the fireball-decay probabilities for a total pion multiplicity of $2i$ or $2i-1$ pions. Thus, the probability of finding $2n$ charged pions among the decay products of a fireball decaying into a total of $2i$ pions is given by

$$P_\beta(2n, 2i) = (\tfrac{2}{3})^n (\tfrac{1}{3})^{i-n} \left[\frac{i!}{n!\,(i-n)!}\right]$$

with a similar expression for $P_\beta(2n, 2i-1)$.

For each value k of the fireball multiplicity p_{k+} and p_{k-} are calculated from Eq. (28) as are the corresponding overall c.m. energies $E_{k\pm} = \gamma_F(E'_k \pm \beta_F p'_k)$. The longitudinal rapidities corresponding to the fastest and slowest fireball-decay products in the overall c.m. frame resulting from decay multiplicity k are then calculated from

$$y_{k+} = \tfrac{1}{2} \ln\left(\frac{E_{k+} + p_{k+}}{E_{k+} - p_{k+}}\right)$$

and

$$y_{k-} = \tfrac{1}{2} \ln\left(\frac{E_{k-} + p_{k-}}{E_{k-} - p_{k-}}\right).$$

Next, the longitudinal momenta corresponding to the bin boundaries $y(i)$ between y_{k+} and y_{k-} are calculated from

$$p_l(k, i) = (E'_k/\gamma_F) \tanh[y(i)] / \{1 - \beta_F \tanh[y(i)]\}.$$

Assuming that charged secondaries are distributed isotropically in the fireball c.m. frame, the contribution of a $2n$ charged-pion decay of a fireball with total decay multiplicity $k \geq 2n$ to the occupation probability of the longitudinal rapidity distribution bin $y(i+1) - y(i)$ lying between y_{k+} and y_{k-} is then given by [taking the first bracketed term of Eq. (29), which corresponds to a one-fireball event with the fireball associated with the target nucleon, as an example]

$$N(i) = P_\alpha(x_{i_B}, x_{i_T}, \xi_{j_T}{}^2) P_\beta(2n, k) \times k[p_l(k, i+1) - p_l(k, i)] / 2\gamma_F p'_k.$$

The summation of all such contributions from each individual term in the brackets in Eq. (29) then gives the occupation probability for charged final-state pions in each c.m. rapidity bin, assuming that all fireball-decay products are pions.

The number density of charged pions per unit of rapidity is then calculated at the center point of each bin. In this model, one half of the total charged-pion number density gives the number density of positive or negative pions per unit of rapidity. In Fig. 1, the calculated number densities of positive or negative pions per unit of rapidity (the two curves are identical) at a c.m. energy of 19.42 GeV (laboratory momentum 200 GeV/c) in nucleon-nucleon scattering are shown as connected by a solid line drawn by eye through the calculated data points. Because the c.m.

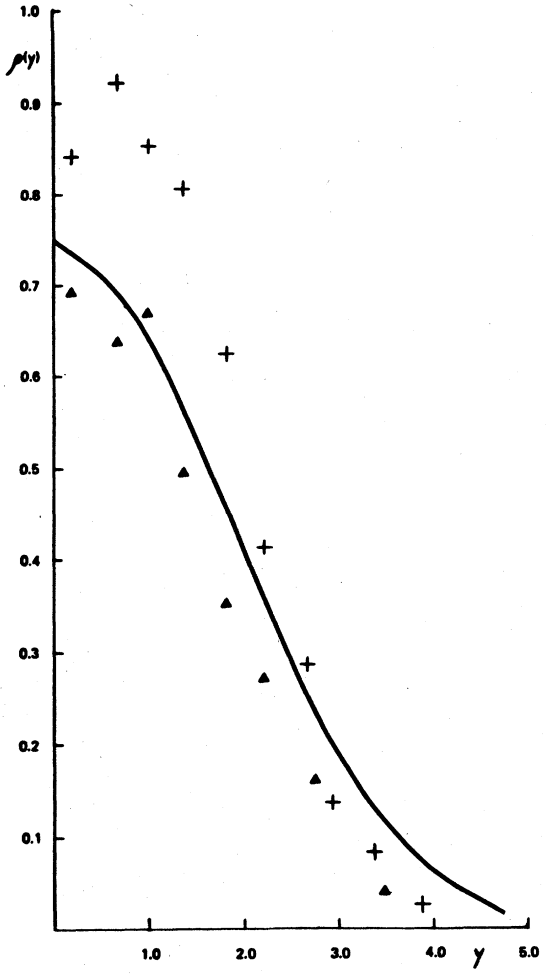

FIG. 1. The solid curve shows the calculated longitudinal-rapidity distribution of final-state π^+ or π^- mesons (the two curves are identical) in nucleon-nucleon scattering at a c.m. energy of 19.42 GeV (incident laboratory proton momentum of 200 GeV/c). The pluses denote the experimental points for the π^+ rapidity distribution and the solid triangles denote the experimental points for the π^- rapidity distribution as taken from Ref. 25.

rapidity distribution is symmetric around $y = 0$ in the nucleon-nucleon c.m. frame, only the forward half of the charged-pion rapidity distribution is shown in Fig. 1. In addition to the calculated curve, Fig. 1 shows the experimental data points for the π plus rapidity distribution (denoted by pluses) and for the π minus rapidity distribution (denoted by solid triangles) as taken from Ref. 25. The agreement with experimental data is quite reasonable.

In preparing Fig. 1, three-point Gaussian integration ($N = M = 3$) was used for numerical integration over the internal-momentum distributions in order to speed up the calculation. Nevertheless, a calculation of the rapidity distributions requires about a minute of machine time on a CDC 6600, so, in the light of my limited resources, I have not calculated the rapidity distributions at all energies.

REMARKS ON HADRONIZATION IN LARGE-TRANSVERSE-MOMENTUM JETS

The model described in this paper does not include a detailed description of the force between colliding quarks and therefore cannot shed light on the angular distribution of scattered quarks and secondary hadrons (or the total quark and hadron cross sections). However, the fireball-decay model of hadronization predicts that a hard-scattered quark will develop into a jet of hadrons with an average momentum transverse to the jet axis of 360 MeV/c. Because of the seagull effect discussed in Ref. 1, the average transverse momentum measured in large-transverse-momentum jets will be larger than this if soft particles are excluded. Furthermore, the following discussion of fireball generation in large-transverse-momentum scattering suggests that the charged multiplicity of large-transverse-momentum jets should increase as the square root of the total jet energy E_j in the rest frame of the two large-transverse-momentum jets resulting from a hard-scattering event.

A large-transverse-momentum jet is assumed to evolve from a quark in one of the colliding hadrons which is scattered through a large angle by a collision with a quark in the other incident hadron. The momentum of this parent quark in the rest frame of the two large-transverse-momentum jets generated by a hard-scattering event is

$$|p_j| = (E_j^2 - m_Q^2)^{1/2}$$

immediately after the hard-scattering event. m_Q is the effective mass of the quark, which is taken as one third the nucleon mass. Let χ denote the change of momentum which arises from the action of the color force between the hard-scattered quark and the spectator quarks which accompanied it in the colliding hadron from the moment of collision until the time when an additional $Q\bar{Q}$ pair is formed out of the potential energy of interaction between the two systems.[1] Then, the total momentum of the $Q\bar{Q}$ system which will evolve into the large-transverse-momentum jet is $p_j' = p_j - \chi$ and the invariant mass m_J^* of the jet system can be found from

$$(p_j - \chi)^2 + m_J^{*2} = p_j^2 + m_Q^2 .$$

Therefore, $m_J^{*2} = 2\chi p_j - \chi^2 + m_Q^2$ and since $p_j \approx E_j$ we have $m_J^* \propto E_j^{1/2}$. Then, if it is assumed that the average number of hadrons produced in a jet is $\langle n \rangle = m_J^*/(p_H^2 + m_\pi^2)^{1/2}$, the average number of charged hadrons produced in a jet is approximately $\langle n_c \rangle \approx \frac{2}{3} m_J^*/(p_H^2 + m_\pi^2)^{1/2}$ which is proportional to $E_j^{1/2}$.

Although the range of jet energies presently accessible to experiment is not adequate to test this prediction, I calculated the fireball decay-multiplicity distributions for large-transverse-momentum jets with jet energy E_j equal to 6.1, 8.0, and 10.05 GeV for comparison with the experimental results from Ref. 26. The results, shown in Table VI, are for $\chi = 0.65$ GeV/c, which is not too different from the corresponding value of 0.54 GeV/c appropriate to jets in e^+e^- annihilation.[1] The calculation assumes that the number n of additional hadrons produced by the initial excited $Q\bar{Q}$ pair (fireball) which generates the large-transverse-momentum jet follows a Poisson distribution truncated at $n_{\max} = (m_J^*/m_{\pi^0}) - 1$ with

$$\langle n \rangle = [m_J^*/(p_H^2 + m_\pi^2)^{1/2}] - 1$$

in analogy to Eqs. (5) and (6). An equation similar to Eq. (15) was then used to obtain the charged-hadron multiplicity distribution of the jet.

CONCLUSION

This paper shows that a simple quark model, using input values which are readily obtained from experiment, can provide a reasonable description

TABLE VI. Comparisons of calculated values of charged multiplicity of large-transverse-momentum jets with $\chi = 0.65$ GeV/c and average transverse momentum of jet hadrons with respect to the jet direction = 0.360 GeV/c with experimental values. Experimental data are taken from Fig. 23 of Ref. 26.

Jet energy (GeV)	6.1	8.0	10.05
Experimental value of $\langle n_c \rangle$	4.10	4.50	5.50
Calculated value of $\langle n_c \rangle$	4.15	4.75	5.33

of many features of nucleon-nucleon scattering events.

(1) The percentage of elastic scattering is constant at high energies and rises at low energies.

(2) The longitudinal rapidity distribution is reasonable.

(3) The model predicts a constant value of the average component of the secondary-hadron momentum transverse to the "jet axis," i.e., the direction of momentum of the secondary-hadron fireball. If the angular distribution of scattering products were considered in the model, the average momentum of secondaries transverse to the beam direction should rise slowly with energy because of the admixture of large-transverse-momentum hard-scattering events.

(4) The behavior of the average charged-hadron multiplicity in nucleon-nucleon scattering is in good agreement with experiment, and the higher moments of the charged-hadron multiplicity distribution generally show the same qualitative behavior as is observed experimentally.

One shortcoming of the model in its present form is that the charged-hadron multiplicity distributions in inelastic scattering are too narrow. This is evidenced by the low numerical values of the higher moments of the multiplicity distribution as compared to experiment. The following effects, which must be included in a more realistic model, will further spread out the distribution of the values of m_F^* and thus widen the charged-hadron multiplicity distributions: (a) using different momentum distributions for the u and d quarks, (b) considering nonmassless exchange between the scattering quarks, and (c) removing the restriction to one-dimensional scattering, which will allow kinematic variations of m_F^*. However, the most important factor leading to a widening of the charged-hadron multiplicity distribution is likely to be a realistic treatment of the variation of the longitudinal momentum transfer Δ as a function of the impact parameter of the colliding constituent quarks. An adequate impact-parameter representation of the constituent-quark scattering could also lead to a calculation of the quark-quark collision cross section, and therefore, through the additivity assumption, a calculation of the nucleon-nucleon total cross section. To indicate the potential magnitude of this effect, calculation 1 was repeated at a c.m. energy of 27.6 GeV with three-point numerical integrations over the internal-momentum distributions ($N=M=3$). This repeat calculation arbitrarily assumed that

$\Delta = 0.9$ GeV/c with probability $\frac{1}{3}$,

$\Delta = 1.8$ GeV/c with probability $\frac{1}{2}$,

$\Delta = 3.6$ GeV/c with probability $\frac{1}{6}$,

so that the average value of Δ remained at 1.8 GeV/c. The results, as shown in Table VII, reveal that the multiplicity distributions have become wider and the resulting values of the calculated parameters are in reasonable agreement with experiment, except for the correlation function f_2 which is roughly 25% low.

In its present form, calculations with this model can be performed relatively cheaply on a computer. I would be happy to correspond with or to assist anyone who might be interested in developing this model further.

Simple extensions of the model, which would slightly increase the computational complexity, include: (i) using different momentum-distribution functions for the u and d quarks to get better agreement with the results of lepton-nucleon deep-inelastic-scattering data, (ii) taking account of nonmassless exchanges between colliding constituent quarks, and (iii) taking account of color and flavor degrees of freedom to include the production of final-state hadrons other than nucleons and pions.

A more elaborate extension, involving some change in the conceptual framework of the model, would require the development of a convenient mathematical representation for the force between two colliding quarks (perhaps inspired by quantum chromodynamics) and some assumptions regarding the breakup of a colliding hadron when one of its constituent quarks undergoes a hard scattering. Such an extension could potentially lead to a calculation of the quark-quark and hadron-hadron cross sections, the angular distribution of final-state hadrons and the charac-

TABLE VII. Results of a calculation employing a distribution of values for the longitudinal momentum transfer as compared to experimental proton-proton inelastic-scattering data taken at a c. m. energy of 27.6 GeV. The experimental data are taken from the same source as in Table I.

Parameter	$\langle n\rangle$	D_2	D_3	D_4	f_2	$\langle n^2\rangle/\langle n\rangle^2$	$\langle n^3\rangle/\langle n\rangle^3$	$\langle n^4\rangle/\langle n\rangle^4$
Experimental value	8.83	4.59	4.09	6.20	12.2	1.25	1.84	3.05
Calculated value	8.74	4.29	4.11	6.01	9.65	1.24	1.83	3.08

teristics of hadron production in large-transverse-momentum jets.

ACKNOWLEDGMENTS

I am very grateful for the continual help, support, and encouragement provided by Lou, John, and Michael Mongan. The initial impetus to develop this model was provided by Paul du T. Van der Merwe many years ago in Munich. Professor Leon Kaufman gave me some valuable assistance in the early phases of the work.

[1]T. R. Mongan, Phys. Rev. D 20, 1093 (1979).

[2]T. R. Mongan, Phys. Rev. D 21, 1431 (1980).

[3]G. Altarelli, N. Cabibbo, L. Maiani, and R. Petronzio, Nucl. Phys. B69, 531 (1974).

[4]T. R. Mongan, Phys. Rev. D 22, 1538 (1980).

[5]Since the model is developed in the c.m. frame for simplicity, the model is not relativistically covariant.

[6]It is assumed that inelastic collisions involve only longitudinal momentum transfer because the great majority of inelastic high-energy hadronic scattering events produce narrow jets of secondaries along the directions of the incident hadrons, and the transverse motion of these secondaries can be neglected in the first approximation.

[7]E. M. Levin and L. I. Frankfurt, Zh. Eksp. Teor. Fiz., Pis'ma Red. 2, 105 (1965) [JETP Lett. 2, 65 (1965)]; H. J. Lipkin and F. Scheck, Phys. Rev. Lett. 16, 71 (1966).

[8]The Poisson distribution is chosen because of its simplicity and because the following assumptions regarding the occurrence of gluons in the color field around a valence quark seem reasonable: (1) The probability of finding a gluon in an infinitesimal volume δV is approximately $\lambda\delta V$, where λ is a small parameter. (2) The probability of finding two gluons in a volume δV is negligible compared to $\lambda\delta V$. (3) The number of gluons in any infinitesimal volume element is independent of the number in any nonoverlapping volume element. These assumptions can be used to derive the Poisson distribution.

[9]D. H. Perkins, Argonne National Laboratory Report No. ANL-HEP-PR-76-54, 1976 (unpublished).

[10]The interaction between nucleons is modeled by an impulsive force in the c.m. frame because the colliding quarks are Lorentz contracted disks of infinitesimal thickness moving at infinite momentum. Therefore, the collision time, defined as the time required for the disks to pass through each other is infinitesimal and an impulsive force may provide a reasonable representation of the force between the colliding systems. Furthermore, at all energies high enough so that the colliding hadrons (or quarks) are moving at essentially infinite momentum, the collision will look the same in the c.m. frame, and the same impulsive force may be used to describe the interaction between the colliding hadrons (or quarks) at all such energies. The impulsive force represents the quark-quark scattering force which might be mediated, for example, by exchange of a gluon carrying no net color charge [Yoichiro Nambu, Sci. Am. 235, No. 5, 48 (1976)]. The dominance of high-energy hadronic scattering by exchange of a zero-mass spin-one object (e.g., a colorless gluon) is also suggested by Regge-pole theory.

[11]A Poisson distribution is again assumed because of its simplicity and because the assumptions given in Ref. 5 also seem reasonable when applied to the probability of producing additional pions within a fireball.

[12]Two arguments based on the uncertainty principle can be used to indicate the approximate size of $|\vec{p}_H|$. The first argument rests on the assumption that the secondary hadrons are created within a fireball having typical hadronic dimensions. The second argument assumes that pions are created from the quarks and antiquarks in a fireball when these energetic quarks and antiquarks move apart and additional $Q\bar{Q}$ pairs are created out of the potential energy of their interaction. Thus, the characteristic volume within which secondary pions are created is related to the distance between a quark and an antiquark at which it becomes energetically favorable to create a $Q\bar{Q}$ pair out of the potential energy between them.

[13]M. M. Malone and S. Y. Lo [Phys. Rev. D 16, 2184 (1977)] have summed the longitudinal momenta of final-state particles in the right-hand hemisphere of the c.m. system for inelastic pp scattering at various energies, thereby determining p'. Their results indicate that $\Delta = 1.8$ GeV/c at $E_{\text{c.m.}} = 45$ GeV.

[14]G. Miller *et al.*, Phys. Rev. D 5, 528 (1972).

[15]G. Berlad and A. Dar, Technion Report No. PH-76-69 (unpublished).

[16]J. Benecke, T. T. Chou, C. N. Yang, and E. Yen, Phys. Rev. 188, 2159 (1969).

[17]G. B. Yodh, lectures at Gif-sur-Yvette school, 1978 (unpublished).

[18]E. Albini *et al.*, Nuovo Cimento 32A, 101 (1976).

[19]R. H. Dalitz, in *Few Body Dynamics*, edited by A. N. Mitra (North Holland, Amsterdam, 1976), p. 636.

[20]*Handbook of Mathematical Functions*, edited by M. Abramowitz and A. Stegun (Dover, New York, 1965).

[21]S. Dado *et al.*, Phys. Rev. D. 20, 1589 (1979).

[22]W. Thome *et al.*, Nucl. Phys. B129, 365 (1977).

[23]R. R. Wilson, Sci. Am. 242 (No. 1), 42 (1980).

[24]R. Hagedorn, *Relativistic Kinematics* (Benjamin, New York, 1963).

[25]J. Whitmore, Phys. Rep. 10C, 273 (1974).

[26]L. di Lella, review talk given at the Xth International Symposium on Multiparticle Dynamics, Goa, India, 1979 [CERN Report No. CERN-EP/79-145, 1979 (unpublished)].